

# Smart Building Creation in Large Scale HVAC Environments through Automated Fault Detection and Diagnosis

Maitreyee Dey<sup>a</sup>, Soumya Prakash Rana<sup>a</sup>, Sandra Dudley<sup>a</sup>

<sup>a</sup>*School of Engineering,  
London South Bank University, London, United Kingdom*

---

## Abstract

Modernisation and retrofitting of older buildings has created a drive to install Building Energy Management Systems (BEMS) that can assist building managers in paving the way for smarter energy use and indirectly, using appropriate methods, occupant comfort understanding. BEMS may discover problems that can inform managers of building maintenance and energy wastage issues and in-directly, via repetitive data patterns appreciate user comfort requirements. The main focus of this paper is to describe a method to detect faulty Heating, Ventilation and Air-Conditioning (HVAC) Terminal Unit (TU) and diagnose them in an automatic and remote manner. For this purpose, a typical big-data framework has been constructed to process the very large volume of data. A novel feature extraction method encouraged by Proportional Integral Derivative (PID) controller has been proposed to describe events from multidimensional TU data streams. These features are further used to categorise different TU behaviours using unsupervised data-driven strategy and supervised learning is applied to diagnose faults. X-means clustering has been performed to group diverse TU behaviours which are experimented on daily, weekly, monthly and randomly selected dataset. Subsequently, Multi-Class Support Vector Machine (MC-SVM) has been employed based on categorical information to generate an automated fault detection and diagnosis system towards making the building smarter. The clustering and classification results further compared with well-known and established algorithms and validated through statistical measurements.

*Keywords:* Heating, Ventilation and Air-Conditioning, Terminal Unit, Big Data, Feature Extraction, Machine Learning, Automatic Fault Detection and Diagnosis

---

## 1. Introduction

Large urban buildings play an enormous role in energy consumption and are crucial focal points in future smart grid efforts. Enabling technologies that can understand building energy profiles, remotely identify faults, reduce energy and user discomfort without the need of resident experts will form part of the smart architecture where energy can be saved, moved to and utilised in a more appropriate way depending on the time of day, year etc. Understanding large buildings play a vital role here, because they are now far more complex, energy consuming systems comprising several elements for example: Heating, Ventilation and Air-Conditioning (HVAC), lighting, power and control systems etc. These environments are also where people spend a vast amount of their day and finding ways to indirectly understand comfort drives energy profile changes in addition to in-house well-being initiatives [1].

Equipment failure and performance degradation of HVAC systems in commercial buildings often go unnoticed until such occurrences cause negative impact on occupant comfort, triggers an equipment-level alarm, deteriorates equipment life or results in excessive energy consumption and

15 Overhead operational costs (OPEX). Therefore, buildings are installed with Building Energy Man-  
16 agement System (BEMS), which are defined as an IT-based solution capable of sensing, control,  
17 and automation hardware to direct automated and/or manual improvements to system operations  
18 utilizing the multi-streams data. It is a rapidly rising market, with BEMS revenues for hardware,  
19 software and services anticipated to upswing from today's \$2.7 billion universal to \$12.8 billion by  
20 2025 [2].

21 This work focuses on the experimental application of machine learning in a real building's HVAC  
22 terminal unit (TU) data to detect and diagnose equipment failures, provide significant energy savings  
23 through pre-emptive maintenance, behaviour analysis and predictive building identification. Large  
24 volumes of rapidly generated TU data is always a challenging study, therefore, dedicated research is  
25 being carried out to analyse big data and develop a machine learning based approach to construct  
26 an Automatic Fault Detection and Diagnosis (AFDD) system. The algorithm employs a data  
27 driven approach and tie together the hidden information buried from big historical building data.  
28 The expected outcome of this research is remote TU fault identification and generating automatic  
29 notification to the building manager which leads to save the energy consumption.

### 30 *1.1. Literature Review*

31 HVAC systems have evolved enormously and significant development has been made in terms  
32 of data mining techniques for fault detection and diagnosis (FDD). HVAC research studies began  
33 in 1980's [3, 4], but from the beginning, practical limitations like scalability and complexity have  
34 made FDD extremely challenging. Based on this survey, the FDD techniques have been categorised  
35 into three major parts: model based, rule based and data-driven based approaches.

36 In model based approaches the data generated from plants and industries are simulations via  
37 mathematical models. In [5], physical laws were employed to derive the first principle model that  
38 signifies the dynamic nature of the system, which is not suitable for real time applications because  
39 such scenarios require fast controller responses. To further reduce the computational cost, a modified  
40 physical model was proposed by Shaw et.al [6]. Later this model incorporated real time HVAC  
41 applications [7, 8]. There are a number of researchers who have proposed the gray-box model  
42 which is a non-complex model to reduce the computational cost of the system and few systems are  
43 proposed to handle the limitations of gray-box model [9, 10]. A Black-box model was proposed  
44 for system identification based on mathematical modelling and has been found to be suitable for  
45 online FDD. Wu and Sun [11, 12] improved the performance of the black-box model for real time  
46 implementation based on parametric and multi-stage regression models, and were able to predict  
47 room temperature in office buildings.

48 Rule-based or Knowledge-based perspective for FDD in HVAC systems is applicable when there  
49 is insufficient data available to employ building mathematical models. This type of method is also  
50 applicable for large scale, complex HVAC systems, and requires a high level of expert knowledge  
51 on a system's fault features [13]. There are three different techniques: casual analysis, pattern  
52 classification, and expert systems that have been already developed for Air Handling Unit (AHU).  
53 Signed Directed Graph (SDG) is proposed for casual analysis by employing the fault symptoms  
54 without first principles [14]. The expert knowledge of a system can be implemented using some  
55 rules and the process can be divided into three types, (a) a system with partial knowledge by  
56 framing IF-THEN rules, (b) a system with deep-expert knowledge involved functional reasoning,  
57 and (c) systems with machine learning capabilities. Schein et. al., [15] developed a FDD system  
58 for operational control with partial or limited knowledge by setting up IF-THEN rules for an AHU.  
59 Manufacturers have effectively verified this concept for real time building applications [16, 17].  
60 Schein and Bush [18] expanded the concept by proposing hierarchical rules for FDD. Yet, expert

61 knowledge based techniques are limited when real data is unavailable. To resolve this restriction,  
62 machine learning methods like Hidden Markov Model (HMM) [19], Kernel Machines (KM) [20]  
63 are applied, where knowledge is automatically extracted from data. Pattern classification based  
64 algorithms are used to build non-linear correlations between data patterns and fault classes in the  
65 absence of clear model structures. Some popular pattern classification based methods are Bayes  
66 Classifier [21], Artificial Neural Networks (ANN) [20, 22], Support Vector Machine (SVM) [23],  
67 Fuzzy Logic [24].

68 Data-driven based techniques build relationships between data patterns and faulty classes of  
69 a system [25]. These approaches extract the key data components and transform the dimension  
70 of the entire data. These key components are then used instead of the whole dataset for FDD.  
71 This approach is appropriate for modern HVAC systems being used in huge commercial buildings.  
72 There are two types of categories for this approach: Signal based FDD and Multi-Variable Statis-  
73 tics (MVS) based FDD. Some existing signal based procedures are wavelet transformation and  
74 short-time Fourier analysis [26]. A combined method using wavelet transformation and principle  
75 component analysis (PCA) is proposed to diagnose faults for air handling unit (AHU) system [27].  
76 It detects faults in large systems using a dimensionality reduction technique that maps the data to  
77 a lower dimensional space. In practice, this FDD methodology is appropriate for fault detection  
78 instead of fault diagnosis. To solve these limitations, integrated or hybrid approaches are considered  
79 for efficient FDD applications in large buildings [28].

80 All of these above stated approaches are limited to particular fault categories (e.g. fan failure,  
81 valve stuck) or fixed data. BEMS data analysis novella recent problem, indeed characterising  
82 Terminal Unit behaviour has not been given much attention in the research hitherto. Thus, this  
83 paper emphasises on TU behaviour analysis.

84 The paper is structured as follows: Section 2 outlines the motivation for this work and provides  
85 detail and context on Terminal Units and their associated problems. Section 3 focuses on the  
86 proposed methodology and imparts details about the feature extraction technique proposed along  
87 with the Clustering and Classification methodologies. Section 4 gives the discussion of experimental  
88 set-up and detailed data acquisition and analysis. The different TU behaviour patterns obtained  
89 as a result of the clustering and further classification result analysis with validation is presented in  
90 Section 5. Section 6 concludes the paper and provides the future research directions of this work.

## 91 **2. Structural Information of HVAC TU**

92 The data is collected for TU fan coil units (FCU) from a real building in central London, UK. The  
93 floor plan drawing of this building is observed closely to understand relationships between HVAC  
94 TUs, rooms, spaces, and other physical features at one level of a structure. The floor plan presented  
95 in Figure 1 shows the position of ground floor FCUs, which are marked with a red line border. There  
96 are 44 FCUs in the ground floor and the whole building comprises of 731 FCUs. These units are  
97 explicit subcomponents of HVAC systems set up in residential, commercial, industrial buildings and  
98 are responsible for the final delivery of comfort inside built environments.

99 A TU is a device consisting of a heating coil, cooling coil and a fan. It is normally ceiling-  
100 mounted and monitored by local thermostats. It may either recirculate internal air, or introduce  
101 fresh air along with re-circulated air. Generally inside buildings, there is a central chiller and boiler  
102 plant that distributes cold water to all the cooling coils and hot water to all the heating coils. If  
103 the environment becomes too warm, the thermostat senses this and signals the chilled water valve,  
104 with cold water then passed through the coil, extracting the heat from the air being blown by the  
105 fan. If it gets too cold depending on the local set point, the heating coil start working in the same  
106 way. A typical schematic of a TU is shown in Figure 2.

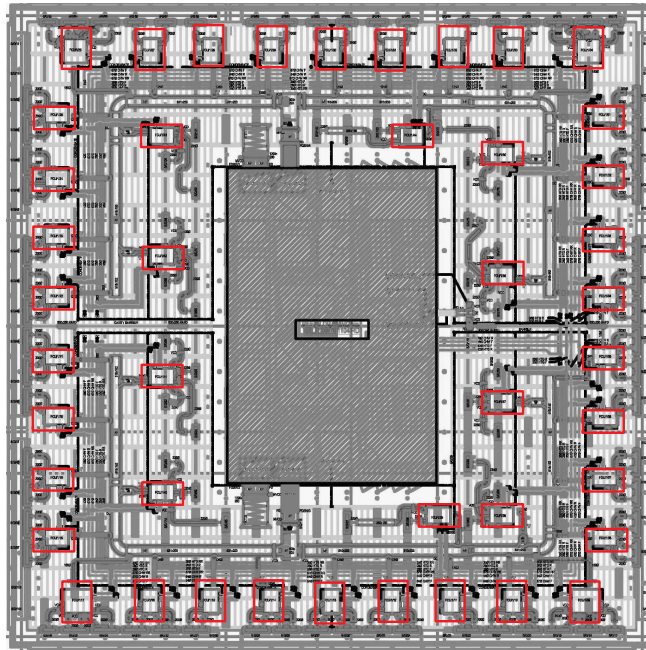


Figure 1: Floor plan architecture of a building in a central London

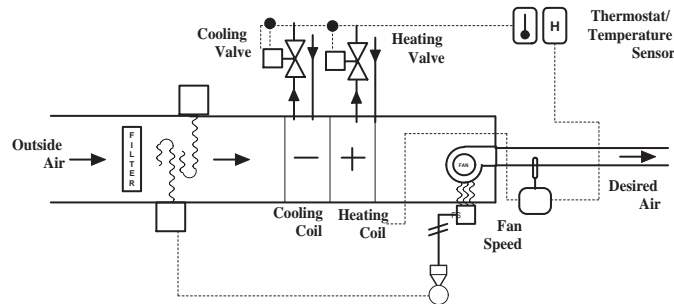


Figure 2: TU schematic diagram

107 The data thus gathered from the TUs inside building exhibit hidden information related to  
 108 building behaviour. A single TU consist of various data streams are as follows:

- 109 • Control temperature [ $^{\circ}\text{C}$ ], frequently measured by each TU or in some cases a zone space  
 110 temperature is used.
- 111 • Set point temperature [ $^{\circ}\text{C}$ ] is the desired or target control temperature of the unit is set by  
 112 the operator or the administrator based on the current demand.
- 113 • Deadband is the control temperature band or range within the process and create two separate  
 114 outputs of heating and cooling set point.
- 115 • Heating and cooling valve or damper actuator control and feedback signals.
- 116 • Enabled signal to indicate the hours of operation.

117 Poorly controlled or faulty TUs such as FCUs can be responsible for significant energy wastage  
 118 and occupant discomfort. For example, a faulty fan coil unit can signal a false heating demand

119 to the boiler, causing the ancillary equipment to activate and begin distributing hot water causing  
120 rooms to overheat. In the following subsection, different TU issues are explained which might cause  
121 faulty behaviour.

### 122 *2.1. Potential TU Issues*

123 There are a number of potential issues that can be identified from TU data analysis. Various  
124 behavioural metrics like saturation, on-ness and hunting can be studied for different TUs to identify  
125 the prevailing issues.

- 126 1. Saturation can be defined as the proportion of time over a day that the valve or damper  
127 is open at maximum. Thus the higher the value, the longer a heating or cooling valve (or  
128 damper) is open.
- 129 2. On-ness can be defined as the proportion of time that a terminal unit has any heating or cooling  
130 demand over a 24-hour period (i.e. any time that demand is greater than 0%). Simply put,  
131 it is how long something is on.
- 132 3. Hunting is calculated using the set point, control temperature and is a measure of how much  
133 it fluctuates over a day.

134 Some of the potential issues that can result in faulty TU behaviours are listed as below:

- 135 1. Poor control- Typically, this can happen due to narrow dead bands being set and/or over  
136 aggressive proportional, integral and differential (PID) control. This can result in the TU  
137 frequently switching between heating and cooling.
- 138 2. Poor sensor location- The temperature sensor could be located at a wrong position. For an  
139 instance, in close proximity to heating and/or cooling elements (e.g. back of a drinks cabinet).
- 140 3. Varying set point- The set point may be varied too frequently typically due to occupant  
141 discomfort (e.g. user is changing set point for personal preference).
- 142 4. Out of hour operation- A unit may be found to operate out of hours because either it has simply  
143 been forgotten (manually operated and left) or the operational time schedule is incorrect.
- 144 5. Incorrect TU sizing for actual demand- It can happen that the load is underestimated and  
145 a bigger unit should have been installed. This is found more often in cooling than heating  
146 mode.
- 147 6. TU unable to receive adequate flow or upstream temperatures- The flow temperature from  
148 the boiler or chiller is not sufficiently high or low to condition the space, sometimes due to  
149 over-ambitious temperature compensation.
- 150 7. Stuck-open valve- Often indicated by a saturation value of 1, it could mean the valve was fully  
151 open over a 24-hour period.
- 152 8. Competition from nearby TUs- A TU is trying to heat the space but an adjacent TU near or  
153 in the same space, is trying to cool the same area. This is generally found where there is poor  
154 hierarchical control over a branch of TUs.
- 155 9. Localised effects- This can be caused either due to high solar gains or TU placed very close  
156 to energy-consumption equipment with high internal gains, like an old lighting fixture or  
157 photocopier.
- 158 10. Unachievable set point- Sometimes it can happen that a user adjusts the set-point temperature  
159 to maximum or minimum value that is simply unachievable for that environment.

160 Even though a TU is considered as “simple device” there can be a multitude of issues that  
161 can lead to faulty behaviour and require expert building engineering knowledge to identify and

162 conclude each one of these issues. Manual TU data investigation can be extremely tedious and  
 163 impossible with the ever-increasing amount of building data and the shortage of suitably qualified  
 164 resident building engineers or managers. Hence automating and bringing intelligence to this process  
 165 using data mining and machine learning approaches could be an ideal solution. This work therefore  
 166 proposes a novel, data-driven feature extraction method and subsequent unsupervised clustering  
 167 to identify different TU behavioural patterns without the need of an expert building engineer  
 168 and further supervised classification employed towards making an automatic fault detection and  
 169 diagnosis system for future data prediction.

### 170 3. Proposed Methodology

171 The current explosion of data in volume, recording and attributing, has initiated the expansion  
 172 of many big data platforms along with parallel data analytics procedures. Huge data might  
 173 produce worse performances in data analytics applications. Simultaneously, it has pushed for data  
 174 dimensionality reduction procedures, but not always with better result [29]. The first milestone of  
 175 the work was then to reduce the dimension of the data set. Thus, we emphasize a novel feature  
 176 extraction method [30] for transforming the data into a lower dimensional space in a unique way.

177 Figure 3 shows the work flow involved here, comprising of two stages: unsupervised and supervised  
 178 learning. Firstly, the vast data is held in a secure cloud and further applied feature extraction  
 179 method, subsequently clustering is employed to group the similar patterns to identify separate faulty  
 180 and non-faulty TUs. Subsequently, classification is applied through training and testing phases to  
 181 understand fault trends and make useful predictions for fault diagnosis. This method leads to  
 182 handle faults and reduce the energy wastage in a building.

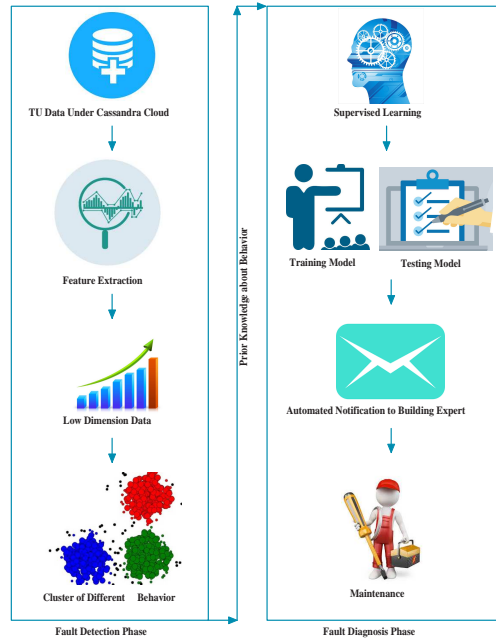


Figure 3: Computational steps involved in proposed methodology

#### 183 3.1. Feature Extraction using TU Data

184 A novel feature extraction method is implemented based on the six different parameters of TU  
 185 data such as, control temperature, set point, deadband, heating effort, cooling effort, and enable

186 signal. The framework for feature extraction creates events by considering the area under the control  
187 temperature and the corresponding power curves which involves three different stages:

- 188 1. Event Discovery Stage
- 189 2. Event Area Calculation Stage
- 190 3. Event Aggregation Stage

### 191 3.1.1. Event Discovery Stage

192 The event discovery is inspired by the Proportional Integral Derivative (PID) controller response  
193 curve [31] as shown in Figure 4, a typical step response curve following a controller responds to a  
194 set point alteration. The curve rises within a period from 10% to 90% of the final steady state value  
195 known as the rise time. Percent Overshoot is the amount that the process variable overshoots the  
196 final value, expressed as a fraction of the final value. Settling time is the time required to settle  
197 within a certain percentage (commonly 5%) of the final value. Steady-State Error is the ultimate  
198 difference between the process variable and set point. Dead time is a delay between when a process  
199 variable changes, and when that change can be observed. For instance, if a temperature sensor is  
200 placed far away from a cold water fluid inlet valve, it will not measure a change in temperature  
201 immediately if the valve is opened or closed. Dead time can also be caused by a system or output  
202 actuator that is slow to respond to the control command, for instance, a valve that is slow to open  
203 or close.

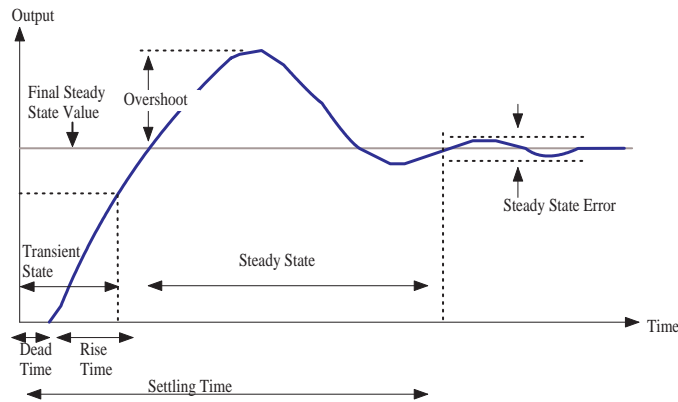


Figure 4: PID controller response curve

204 In this stage, the events are selected using control temperature and corresponding power effort  
205 data streams. Inside a building, when the heating and cooling units are started during normal  
206 operational hours, the temperature changes depending upon the environmental request. Therefore,  
207 two types of events, heating event and cooling event are selected depending on the corresponding  
208 power demand at that time instance. Based on the temperature variations with respect to the set  
209 point value, the data stream is divided into different phases and used to identify different events  
210 that happen in a single day. A single day TU data is being separated into four events as shown in  
211 Figure 5.

- 212 1. Event Start (ES): ES is assumed when the BEMS starts and the time instance when temper-  
213 ature starts to change.
- 214 2. Response Delay (RD): The delay is anticipated when the temperature starts to respond only  
215 after a certain delay from the previous point when the BEMS starts.

- 216 3. Goal Achieved (GA): When the temperature reaches to the desired set point, it is assumed  
 217 as GA. This is basically the time during rise time.  
 218 4. Event End (EE): EE is occurring when the temperature exceeds the dead band.

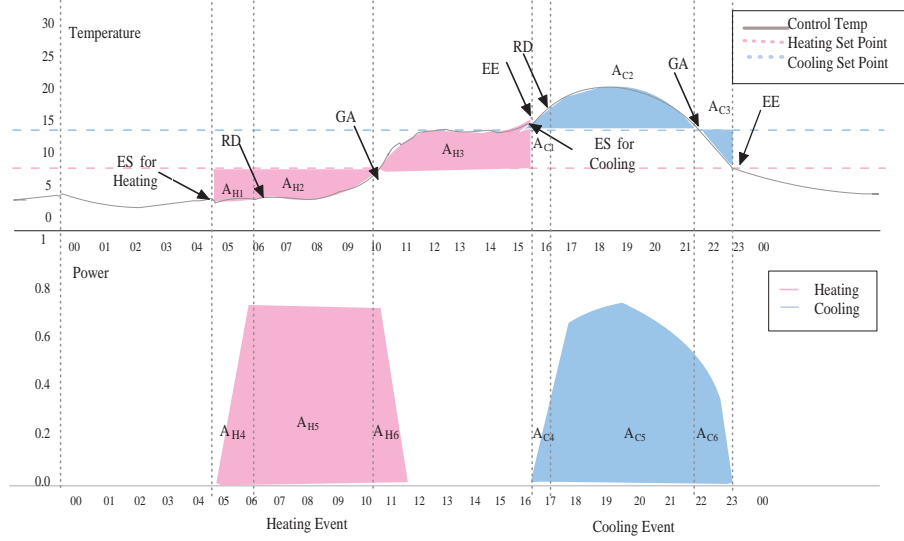


Figure 5: Event discovery process of one day TU

### 219 3.1.2. Event Area Calculation Stage

220 After discovering the appropriate heating and cooling events, the estimated area under the  
 221 temperature and power curve for each event has been calculated. Subject to the event type area  
 222 calculations are carried out respectively for both heating ( $H$ ) and cooling ( $C$ ) events. In effect, six  
 223 areas (three from temperature and three from power curve) for each heating event and similarly,  
 224 six areas for each cooling event are calculated. Altogether twelve different areas are derived from  
 225 all the daily TU data.

226 Equation (1) shows the area ( $A_E$ ) beneath the curve  $f(x)$  at every time interval  $\Delta x$ .

$$A_E = \sum_{i=0}^n f(x_i) \Delta x \quad (1)$$

227 In heating event, the area calculations for temperature are indicated by  $A_{H_1}$  to  $A_{H_3}$  and for  
 228 power indicated by  $A_{H_4}$  to  $A_{H_6}$ . Likewise for a cooling event, the area calculations for temperature  
 229 are indicated by  $A_{C_1}$  to  $A_{C_3}$  and for power are indicated by  $A_{C_4}$  to  $A_{C_6}$ . After these areas have been  
 230 computed, they are normalized to obtain the final feature values as  $F_{H_1}$  to  $F_{H_6}$  and  $F_{C_1}$  to  $F_{C_6}$  as  
 231 denoted by Equations (2) to (5).

232 Equations (2) and (3) show the area calculations for a heating event.

$$F_{H_1} = \frac{A_{H_1}}{T_{H_1}}, \quad F_{H_2} = \frac{A_{H_2}}{T_{H_1}}, \quad F_{H_3} = \frac{A_{H_3}}{T_{H_2}} \quad (2)$$

where,  $T_{H_1} = \max(A_{H_1} + A_{H_2})$   
 and,  $T_{H_2} = \max(A_{H_3})$

$$\begin{aligned}
F_{H_4} &= \frac{A_{H_4}}{P_{H_1}}, & F_{H_5} &= \frac{A_{H_5}}{P_{H_1}}, & F_{H_6} &= \frac{A_{H_6}}{P_{H_2}} \\
&\text{where, } P_{H_1} &= \max(A_{H_4} + A_{H_5}) \\
&\text{and, } P_{H_2} &= \max(A_{H_6})
\end{aligned} \tag{3}$$

Equations (4) and (5) show the area calculations for a cooling event.

$$\begin{aligned}
F_{C_1} &= \frac{A_{C_1}}{T_{C_1}}, & F_{C_2} &= \frac{A_{C_2}}{T_{C_1}}, & F_{C_3} &= \frac{A_{C_3}}{T_{C_2}} \\
&\text{where, } T_{C_1} &= \max(A_{C_1} + A_{C_2}) \\
&\text{and, } T_{C_2} &= \max(A_{C_3})
\end{aligned} \tag{4}$$

$$\begin{aligned}
F_{C_4} &= \frac{A_{C_4}}{P_{C_1}}, & F_{C_5} &= \frac{A_{C_5}}{P_{C_1}}, & F_{C_6} &= \frac{A_{C_6}}{P_{C_2}} \\
&\text{where, } P_{C_1} &= \max(A_{C_4} + A_{C_5}) \\
&\text{and, } P_{C_2} &= \max(A_{C_6})
\end{aligned} \tag{5}$$

### 3.1.3. Event Aggregation Stage

Multiple heating and cooling events can occur during a single day therefore, all the events of a given type need to be aggregated to represent the averaged values. So, the next step in the feature extraction process is event aggregation. The final aggregated features can be represented using the Equations (6) and (7), where,  $k$  denotes the number of events and  $n$  denotes total number of occurrences for each event in both the type. Thus, a single day TU data can be represented using twelve features for both the heating and cooling events.

$$F_{H_k} = \frac{1}{n} \sum_{i=1}^n (F_{H_{k_i}}) \tag{6}$$

$$F_{C_k} = \frac{1}{n} \sum_{i=1}^n (F_{C_{k_i}}) \tag{7}$$

### 3.2. Unsupervised Learning

Due to the lack of prior knowledge about the data involved, an unsupervised learning methodology is employed to discover a set of TU behaviours. Here, an extended K-Means (X-means) [32] clustering is employed on the extracted TU features (obtained from the Equations (6) and (7)). This clustering is used to avoid the limitation of conventional K-means clustering, which tried to automatically determine the number of clusters based on Bayesian Information Criterion (BIC) scores. Initially, the whole dataset is considered as single cluster and BIC score is calculated by Equation 9. Now, the conventional K-means is performed by varying cluster seed value. The following steps of X-means are as follows:

**Improve-params (k-means)**- K-means is evaluated by the seed value of cluster number. The objective function used for this work is the Equation 8.

$$J = \sum_{j=1}^k \sum_{i=1}^n \|X_i^{(j)} - \mu_j\|^2 \tag{8}$$

252 Where,  $\|X_i^{(j)} - \mu_j\|^2$  is the Euclidean distance measure between a data point  $X_i^{(j)}$  and the cluster  
 253 centre  $\mu_j$ . It is an indicator of the distance of the  $n$  number of data points from their respective  
 254 cluster centres. The main idea is to define  $K$  centroids, one for each cluster. Each data point is  
 255 assigned to the group that has the closest centroid. After all the data points are assigned, the  
 256 positions of the  $K$  centroids are recalculated. The above steps are reiterated till the centroids no  
 257 longer move.

258 **Improve-structure (BIC)**- In this stage, the BIC score is calculated based the clustering  
 259 outcomes. Maximum likelihood of the current clusters is used to determine the BIC. Centroids are  
 260 broken further based on the BIC score in order to better fitting of the data. The BIC is computed  
 261 here using Equation 9.

$$BIC_{score} = -2\log(L) + K\log(n) \quad (9)$$

where,  $L = P(x | \theta, M)$

262 Where,  $L$  is the maximum value of the likelihood function of the model  $M$ . The other parameters,  
 263  $x$ ,  $\theta$ ,  $n$ , and  $K$  denote the observed data, the parameter of the model, total number of data points  
 264 and the number of free parameter to be estimated respectively.

265 **K>Kmax**- Once centroid ( $k$ ) is determined and  $K$ -means is performed,  $K_{max}$  is then selected,  
 266 and all centroids are tested. As the lower BIC score is always preferred for better fitness of the  
 267 data, then BIC score is compared between  $K$  and  $K_{max}$ . If the current model has a better score,  
 268 then the split is considered the best strategy for clustering.

### 269 3.2.1. Clustering Internal Evaluation

270 Internal validation criteria are used to evaluate the effectiveness of an unsupervised learning  
 271 technique where the external known class labels are not present. This evaluation measures the degree  
 272 of intra-cluster cohesion and inter-cluster separation. Here, Davies-Bouldin (DB) and Silhouette  
 273 (SI) criterion is perform for the evaluation of the clustering technique.

- 274 • **Davies-Bouldin Index**- The Davies-Bouldin index is defined in Equation 10, where,  $\Delta_{i,j}$  is the  
 275 clusters distance ratio for the  $i$ th and  $j$ th within to between cluster.  $\delta_i$  and  $\delta_j$  is the average  
 276 distance between each point in the cluster from the centroid of that  $i$ th cluster and the average  
 277 distance between each point in the  $j$ th cluster and the centroid of the  $j$ th cluster [33].

$$DB = \frac{1}{k} \sum_{i=1}^k \max_{j \neq i} \frac{\delta_i + \delta_j}{\Delta_{i,j}} \quad (10)$$

- 278 • **Silhouette Index**- The silhouette indexing [34] is a measure of the similarity of each point with  
 279 other points in its own cluster, when compared to points in other clusters. The silhouette  
 280 value is defined in Equation 11. Here  $a_i$  is the average distance from the  $i$ th point to the  
 281 other points in the same cluster, and  $b_i$  is the minimum average distance from the  $i$ th point  
 282 to points in a different cluster.

$$SI = \frac{1}{nk} \sum_{i \in k} \frac{b_i - a_i}{\max(a_i, b_i)} \quad (11)$$

283 The silhouette value ranges from -1 to +1. A high value indicates that  $i$  is well-matched to its  
 284 own cluster. The clustering solution is considered appropriate if most points have a high silhouette  
 285 value. Whereas, a low DB value consider the clustering solution is appropriate.

286 *3.3. Supervised Learning*

287 Supervised learning is exercised on the discovered knowledge from clustering. It has training  
 288 and testing phases to adopt and predict different faults. Although several methods are adopted for  
 289 classification, support vector machine (SVM) is a well-known binary classifier but it is modelled  
 290 as a multiclass classifier in the work presented here. Thus, Multi-Class Support Vector Machine  
 291 (MC-SVM) [35, 36] is employed on the extracted TU feature by optimizing the distance between  
 292 support vectors (TUs from different groups) given by Equations (12) and (13).

293 In Equation (12) a set of training pattern is denoted by  $(x_1, y_1), \dots, (x_l, y_l)$  of cardinality  $l$ , where  
 294  $x_i \in R^d$  and  $y_i \in 1, \dots, k$ ,  $w \in R^d$  is the weight vector,  $C \in R_+$  is the regularization constant, and  
 295  $\varphi$  is mapping function which projects training pattern into a suitable feature space  $H$  that allows  
 296 for nonlinear decision surfaces. The constraints  $\xi_i \geq 0, i = 1, \dots, l$ , are implicitly indicated in the  
 297 margin constraints of (12) when  $t$  equals  $y_i$ .

$$\begin{aligned} \min_{w_m \in H, \xi \in R^l} \quad & \frac{1}{2} \sum_{m=1}^k w_m^T w_m + C \sum_{i=1}^l \xi_i \\ \text{subject to} \quad & w_{y_i}^T \varphi(x_i) - w_t^T \varphi(x_i) \geq 1 - \delta_{y_i, t} - \xi_i \\ & i = 1, \dots, l, t \in 1, \dots, k \end{aligned} \tag{12}$$

298 Whereas in Equation (13),  $\delta_{i,j}$ , is the delta (defined as 1 for  $i = j$  and as 0 otherwise). The final  
 299 decision function is defined as,

$$\text{argmax}_m f_m(x) = \text{argmax}_m w_m^T \varphi(x) \tag{13}$$

300 In addition Equation (12) focuses on classification rule (13) without any bias terms. A non-zero  
 301 bias term can be simply exhibited by adding an additional feature to each  $x$ . Therefore, different  
 302 categories of data are classified by solving this decision function and the results are analysed in the  
 303 following section. A pseudo code for the proposed work is presented in the Algorithm 1.

304 *3.3.1. Classification Performance Evaluation*

305 After performing classification the obtained results are evaluated through well-known statistical  
 306 performance metrics, precision and recall for calculating the accuracy of the system. Precision  
 307 calculate the percentage of truly predictive TUs among all the positively detected TUs in the  
 308 dataset and recall measures the relevant outcomes which are detected among the total dataset  
 309 shows in Equations (14) to (15). The performance measurement is based on the number of true  
 310 positive (TP), false positive (FP), and false negative (FN). TP is the total number of correctly  
 311 labelled TUs, whereas FP is the total of incorrectly assigned TUs, and FN is the total of not  
 312 labelled as should be belonging to particular classes.

$$\text{Precision} = \frac{\text{TruePositive}}{\text{TruePositive} + \text{FalsePositive}} \tag{14}$$

$$\text{Recall} = \frac{\text{TruePositive}}{\text{TruePositive} + \text{FalseNegative}} \tag{15}$$

---

**Algorithm 1** Pseudo code for proposed AFDD

---

**Require:** Temperature and power feature of TUs =  $\{T_1, T_2, \dots, T_n\}$

```
1: Fault detection stage:
2: Maximum cluster number = Max
3: K = BIC score for previous model
4: Kmax = BIC score for current model
5: for all Max = 2 to 10 do
6:   Assign initial values for means =  $\mu_1, \mu_2, \dots, \mu_{Max}$ 
7:   Assign each TU to the cluster which has closest mean  $\Leftarrow$  using the Eq. 8
8:   Update means
9:   Calculate BIC score for current model Kmax  $\Leftarrow$  using the Eq. 9
10:  if K > Kmax then
11:    return Go to line 5
12:  else
13:    Max is considered as final cluster number & exit loop
14:  end if
15: end for
16: Six groups of labelled patterns = {C0, C1, ..., C5} are produced by X – means
17: Fault diagnosis stage:
18: Train MC – SVM model by 10%, 20%, and 30% data using objective function
19: Make the prediction on rest of TUs
```

---

## 314 4. Experimental Set-Up

315 The present case study is a seventeen floor building in central London, U.K. with seven hundred  
316 and thirty one terminal units distributed across the different floors. Figure 6 shows the developed  
317 system architecture and various stages of our proposed AFDD, which handles data storage, re-  
318 trieval, analysis, visualization, and support for decision making. There are six different parameters  
319 (set point, dead band, control temperature, enabled, heating effort, cooling effort) selected for this  
320 experiment. Based on these parameters the demand and the control strategies are varied and deal  
321 with the real time TU issues as mentioned in section 2.1. These raw data comprise information  
322 e.g. time stamp, voltage, temperature, etc. It has problems, as would be expected in real environ-  
323 ments, of different sampling rates for different attributes, variable arrival time, missing values for  
324 intermediate time stamps, etc. Therefore, the TUs with the missing data are filtered and linearly  
325 interpolated to resample data at regular ten minute time intervals.

### 326 4.1. TU Data Retrieval Process

327 The BEMS data is extracted via a single embedded PC connected to the BEMS network as  
328 a network node (thus the device needs to be given an address on the network - the detail of this  
329 depends on the type of BEMS). Currently a PC Engine 2D13 ALIX embedded PC is used. The  
330 embedded PC is also connected to the Internet using either the buildings existing Internet connection  
331 or through a mobile network router.

#### 332 4.1.1. Data Collection

333 The embedded PC contains embedded software that is used to:

- 334 1. Obtain a map of the BEMS network. This includes all the:

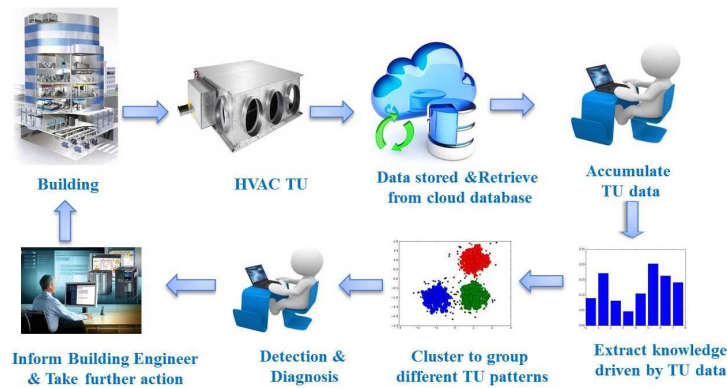


Figure 6: Framework of the experimental TU data retrieval process

- Local Area Networks (LANs) on a BEMS network (a BEMS network is more accurately called internetworks and consists of multiple LANs).
- Devices on a LAN (a single device may relate to one or many pieces of building services equipment).
- Data points on a device. These can be binary or analogue control signals, feedback signals or settings.

For each of the LANs, Devices and Data point the text label and numerical ID is obtained.

2. Polling the values of the data points (typically at intervals of 30 minutes data point type and, by inference, how frequently values are likely to change. For example: the control and feedback signals are polled more frequently while the settings are polled less frequently).
3. Store/buffer the data if the internet connection is lost.
4. Securely send the data to the cloud servers.

#### 4.1.2. Data Characteristics

This BEMS data follows the characteristics of "4V" [37], i.e., volume, variety, velocity, and value which reflects big data characteristics.

**Volume:** The data is continuously generating and increasing the volume. In this experiment, approximately 48 million data points are considered.

**Variety:** The data type is not only traditional structured, but also mixed of structured, semi-structured, and unstructured. There are six types of data are included such as, time stamp, voltage, temperature, binary signal on and off. This complete set of different attributes make a composite structure which needs a complex processing logic to handle the aggregation.

**Velocity:** The speed of the data flow is very fast. These massive and continuous data is stored in Cassandra cloud from the source device. Approximately one million data points are gathered every day for a single building, which helps us to make valuable decisions that provide strategic advantages after handling the data velocity.

**Value:** These data are as valuable as the building outcomes. It enables us to be aware of the behaviour of TUs, which increase the potential to improve fault analysis, decision making capabilities and measure the faulty equipment for diagnosis and energy saving purpose. The proposed work is implemented feature extraction, clustering and classification for decision-making process and to determine the ultimate value of the collected data.

365 4.2. Typical Lab Set up for Parallel Processing

366 The implementation and performance of the proposed method relies on the processing architec-  
 367 ture in place and is shown in Figure 7. The architecture has been set-up for this work comprises  
 368 Apache Spark [38] an open-source cluster computing framework that enables the scalability and  
 369 fault tolerance of Map Reduce using resilient distributed datasets (RDDs). A RDD is a group of  
 370 objects partitioned through a set of machines that can be reconstructed if partition is lost. Spark  
 371 in memory runs up to 100 times faster for certain applications by allowing user programs to load  
 372 data into a clustered memory and querying repeatedly. It is highly suitable for machine learning  
 373 algorithms [39, 40]. Spark requires a cluster manager and a distributed storage system. Here Spark  
 374 version 2.0 is used with 5 CPU core of 8GB memory each is set-up by one master and four workers  
 375 and the connection of the distributed storage with Apache Cassandra interface. The experiments  
 376 have been performed using 64-bit Java version 8.

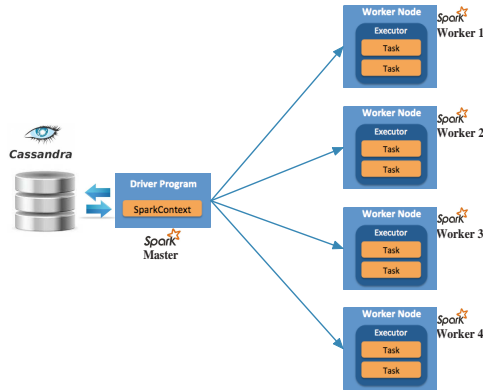


Figure 7: Set-up of parallel processing architecture

377 5. Result Analysis

378 After cleaning and aggregating the data as discussed in the previous section, experiments were  
 379 conducted on four types of data volumes such as, daily, weekly, monthly and randomly selected  
 380 data from the months of July to October (inclusive) 2015. The analysis has been performed on the  
 381 building under test’s historical data to reveal hidden patterns through the employment of machine  
 382 learning. Day analysis was performed on 17th July 2015 TUs, week analysis performed from 17th  
 383 July to 23rd July for 5 working days (excluding weekend) and month analysis done for 22 days  
 384 since weekends have been excluded from the analysis. The random analysis was conducted on the  
 385 randomly selected TUs from July to October 2015. Data details are given in Table 1.

Table 1: Experimental data details

No of Days	Total number of TUs	Operating TUs	Description
1 Day	731	723	17th July, 2015
1 Week, (5 days)	3655	3615	17th to 23rd July 2015 (except 18th and 19th)
1 Month, (21 Days)	15351	15178	17th July to 14th August 2015 (except weekends)
3 Months, (71 Days)	39088	38591	17th July to 23rd October 2015 (except weekends)

386 A new feature extraction algorithm (presented in Equation (2) - (5)) is proposed to reduce,  
 387 measure, and build derived values from these initial datasets intended to be informative and non-  
 388 redundant, which is facilitates subsequent learning and generalization steps. The raw data is trans-  
 389 formed into a 12-dimensional ( $(F_{C_1}$  to  $F_{C_6}$ ) and  $(F_{H_1}$  to  $F_{H_6}$ )) data for each TU. The visualization  
 390 of these multivariate features for a single TU are illustrated by radar in Figure 8. The radar graph  
 391 is a circular display with twelve different quantitative axes. Each axis represents a single feature  
 392 which signifies the fluctuation of temperature and power. The centre of the radar is zero valued  
 393 and the edge point is with maximum value. These feature values are plotted along each axis that  
 394 forms a unique shape and describes TU performance. The proposed feature extraction algorithm  
 395 (described in section 3.1) generates a feature vector of 12 numeric values which contains the cool-  
 396 ing and heating behaviour of a TU. Thus, the radar is being divided into two parts, first six axes  
 397 ( $(F_{C_1}$  to  $F_{C_6}$ )) are represent cooling events and next six axes ( $(F_{H_1}$  to  $F_{H_6}$ )) are represent heating  
 398 events.

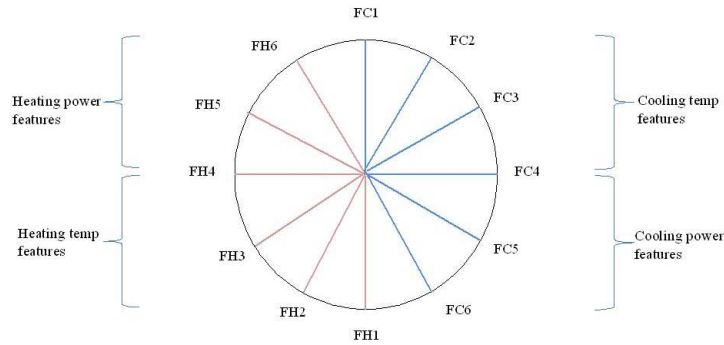


Figure 8: Description of radar graph

399 Here,  $F_{C_1}$  and  $F_{H_1}$  describe the temperature state through the area from the event start (ES)  
 400 to response delay (RD),  $F_{C_2}$  and  $F_{H_2}$  describe the time of response through the area from response  
 401 delay (RD) to goal achieve (GA),  $F_{C_3}$  and  $F_{H_3}$  describe the event end after reaching the set-point  
 402 through the area from goal achieve (GA) to event end (EE). Similarly,  $F_{C_4}$  to  $F_{C_6}$  and  $F_{H_4}$  to  $F_{H_6}$   
 403 represent the power demand for corresponding temperature change. So, it is to be further noted  
 404 that greater areas under GA to EE area represent a “well behaved” TU, because this implies that  
 405 the TU achieves the set point (goal) and spends more time within the dead band (range between  
 406 heating and cooling set point), whereas the area under ES to RD and RD to GA is larger, it denotes  
 407 that the temperature is not within the dead band or takes a long time to reach the set point. The  
 408 more area for power effort indicates the more power consumption which also signifies a “badly  
 409 behaved” TU.

### 410 5.1. Clustering Analysis

411 Now, the TU data with different attributes are present, but the characteristics or possible  
 412 patterns are unknown except for functioning and malfunctioning TUs. Therefore, the X-means  
 413 clustering is performed to find out the possible partitions of the data by varying cluster number  
 414 from 2 to 10 with 6 being found as the optimal number of cluster to describe the distinct TU  
 415 behavioural patterns.

416 Clustering is performed on approximately forty thousand TUs and the visualization of the  
 417 compact groups is shown in the radar graphs below. Figure 9 shows six radars of the daily clustering  
 418 analysis and each radar represents a single TU which is the nearest to that cluster centre to make

419 a generalized conclusion on that group. It is discovered from cluster analysis of TU characteristics  
 420 pattern over daily data (shown in Figure 9), that the heating trend is captured in cluster-3 and  
 421 cooling trends are captured in rest of the clusters. TUs belonging to cluster-0 achieve their set  
 422 point and the feature values are in the third axis ( $F_{C_3}$ ) of the radar. It represents the area under  
 423 GA to EE events for the temperature curve, therefore these TUs exert little power effort and stay  
 424 within their dead band. Cluster-1 represents TUs whose features are in the third axis ( $F_{C_3}$ ) which  
 425 indicates GA to EE state i.e., those TUs require average power (e.g., values are in  $F_{C_6}$  axis) to  
 426 reach the set point. So, TUs belong to cluster-1 use extra power than the TUs are in the cluster-0.  
 427 The TUs of cluster-2 behave similar to cluster-1 but these TUs use higher power levels to reach the  
 428 set point within the buildings operational hours. TUs of cluster-3 capture the area under RD to  
 429 GA ( $F_{C_5}$ ) is large for both the temperature and power curves, which means more heating power is  
 430 required, and the set point is not achieved during working hours. The feature values of cluster-4  
 431 fit in first axis ( $F_{C_1}$ ) which implies time requirement is very large. Thus, area under the ES to RD  
 432 state for both the temperature and power curves indicates that the TUs take longer times and are  
 433 unable to achieve the required set points. For cluster-5, the area under the RD to GA for both the  
 434 temperature and power curves shows the need of high power.

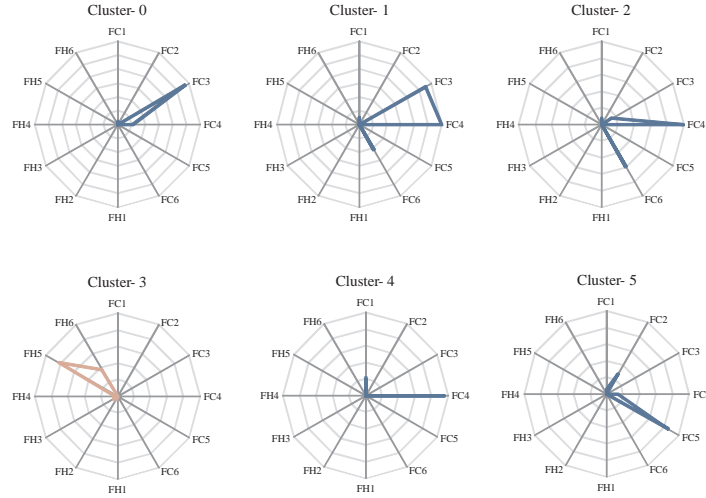
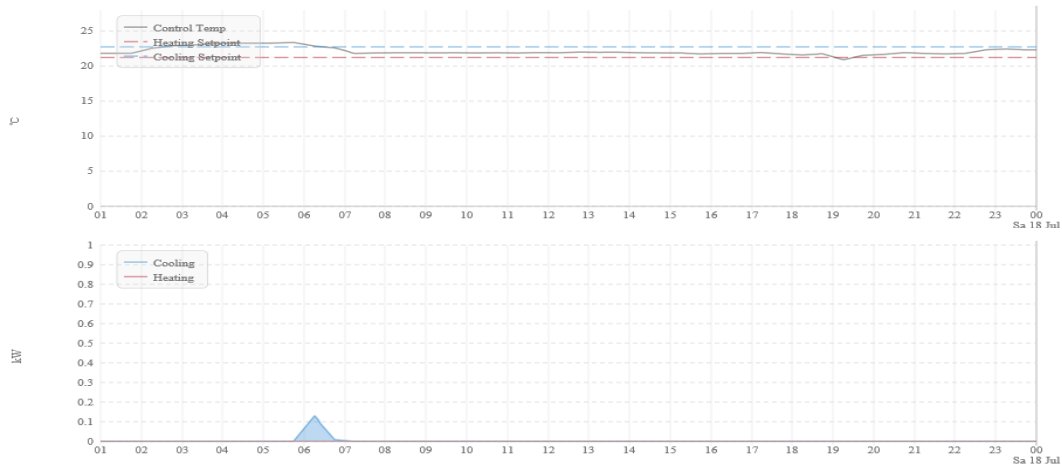


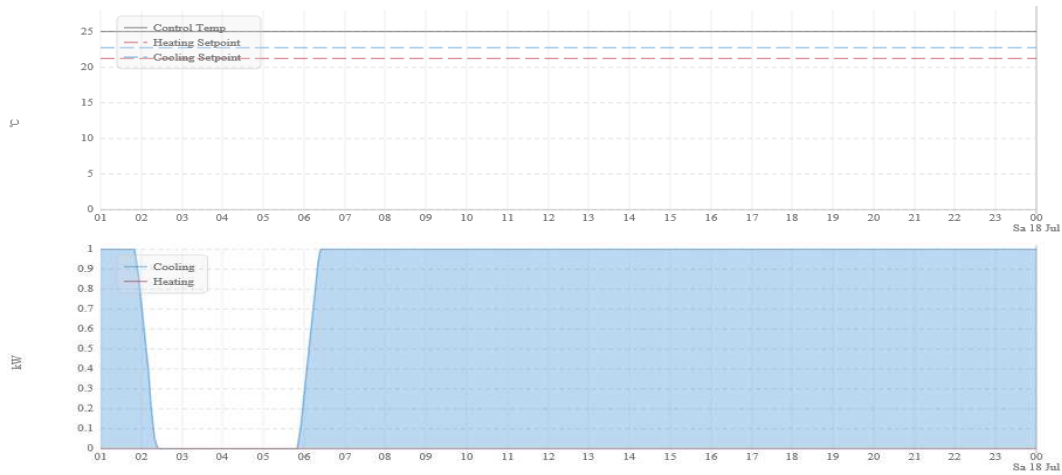
Figure 9: Cluster analysis of Daily TUs

435 Two examples of faulty and non-faulty deemed TUs, obtained from the cluster analysis are  
 436 shown in Figure 10. Figure 10(a) shows cooling non-faulty TU behaviour which belongs to cluster-0  
 437 of Figure 9. This indicates the behaviour where the temperature is consistently held within the  
 438 deadband and low power is consumed during working hours. Figure 10(b) shows a cooling faulty  
 439 TU behaviour which belongs to cluster-4 of Figure 9. Though the TU is exerting maximum effort  
 440 in terms of power consumption, it is still unable to reach the desired set point. In this case it may  
 441 be that the TU is indeed faulty or that the TU is not actually faulty but that the requests made  
 442 of it are unreasonable i.e. poor sensor location (behind a drinks dispense cabinet for example), the  
 443 room is sun drenched or has large unopened windows. Pivotaly, the data shows there is a problem.  
 444 Moreover, this work is not limited to any fixed type of faults; it can detect any kind of abnormal  
 445 behaviour as faulty, where the temperature and power are both or either in an untenable position  
 446 as is the case here.

447 Therefore, the X-means clustering partitioned the daily TU data into 6 groups based on their  
 448 property. It revealed the 6 different hidden patterns of the TUs. These distinct behaviours are



(a) Temperature within dead band with low cooling power



(b) Cooling saturation and on-ness

Figure 10: Example of (a) a non-faulty TU and (b) a faulty TU

449 tabulated in Table 2.

Table 2: Cluster pattern description of daily TUs

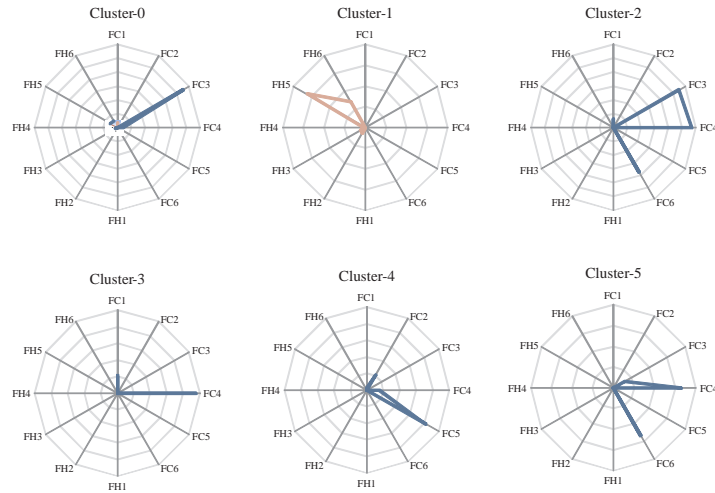
Cluster Number	Description of Clustering Pattern
C-0	TUs that show both heating and cooling characteristics. The desired control temperature is achieved with low power effort, and is done in normal building operating hours.
C-1	These are cooling TUs where the control temperature is achieved within the desired band with medium or average power effort.
C-2	Cooling TUs where control temperature is achieved but with a high-power effort.
C-3	TUs showing control temperature hunting patterns along with medium to high power effort and continuation of this pattern outside operational hours.
C-4	TUs where the control temperature does not achieve the desired set point (out by up to 5 degree C) with high power effort.
C-5	TUs where the control temperature does not achieve the desired set point (out by up to 10 degree C) with high power effort.

Furthermore, this experiment is conducted on the same number of TUs for a week, month, and for random data to check the feasibility, and robustness of the proposed clustering method. Figure 11(a) shows the cluster analysis of TU behaviours during week days, 11(b) for a month, and 11(c) for randomly selected TUs. The repetition of the TU behaviour is found during the clustering experiment on weekly, monthly, and randomly selected data. TUs of cluster-0 of Figure 9, cluster-0 of Figure 11(a), and cluster-3 of Figure 11(b) are found to have similar heating and cooling trends, where goal or desired temperature is achieved with very low power demand. Likewise, the TUs of cluster-1 of Figure 9, cluster-2 of Figure 11(a), cluster-0 of Figure 11(b), and cluster-0 of Figure 11(c) follow similar trends where the set-point is achieved with average power effort. In case of TUs from cluster-2 of Figure 9, cluster-5 of Figure 11(a), and cluster-2 of Figure 11(c) higher power effort are needed to reach the set-point. The hunting behaviour of TUs is found with high power consumption during operational and out of operational hours in cluster-3 of Figure 9, cluster-1 of Figure 11(a), cluster-1 of Figure 11(b), and cluster-3 of Figure 11(c). Likewise the daily TUs of cluster-4 of Figure 9 is similar to cluster-3 and cluster-5 of Figure 11(a) and Figure 11(b), where set-point is not achieved but power is still consumed during out of operational hours. Similar TU behaviours e.g. cluster-5 of Figure 9 is found respectively in cluster-4, cluster-4, and cluster-5 of Figure 11(a), 11(b), and 11(c). It is noted that the patterns found in cluster-2 of Figure 11(b) and cluster-4 of Figure 11(c) are very similar to each other, where set-point is achieved and both captured heating trends. Another two similar heating patterns of TUs are found in cluster-1 and cluster-3 of Figure 11(c), both achieved set-point using average to high power effort.

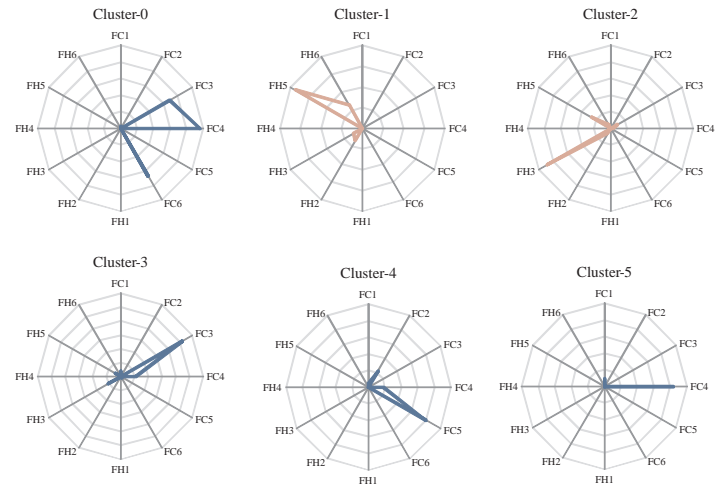
### 5.1.1. Clustering Validation

This initial pattern discovery process is completely unsupervised where no prior label information is available. Internal cluster evaluation criteria (Davies-Bouldin and Silhouette) are used to validate the clustering results and assess compactness of those groups. Also, the proposed X-means results are compared with two different clustering algorithms: Hierarchical clustering and Gaussian mixture model [41] to prove the advantage for using X-means. The quality of the clustering and reason to use X-means is summarized in Figure 12. The comparison and validation results across daily, weekly, monthly and randomly selected TU data are included here.

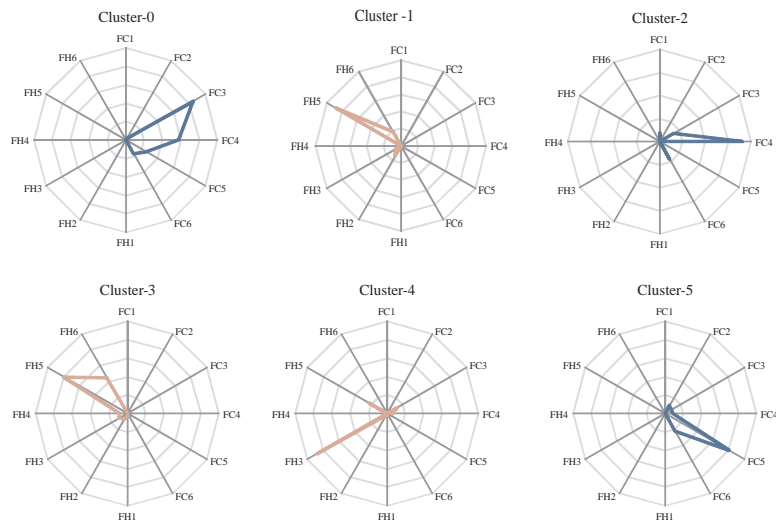
Figure 12(a) demonstrates the DB indexing results of X-means for cluster number 2 to 10 and compared with hierarchical and Gaussian mixture algorithm. As the lowest DB value is preferred, it is seen from the graph that lowest DB value is found when the cluster number is six for the daily, weekly, monthly, and randomly selected TUs for x-means. Similarly, DB values are little higher in case of hierarchical clustering. But heavy fluctuation of DB values of Gaussian mixture model shows the incompactness of the clustering outcomes. Therefore, the lower value of DB in X-means for cluster number 6 shows a good compactness of the clusters than hierarchical clustering. Figure 12(b) shows the SI indexing results for x-means, hierarchical and Gaussian mixture algorithm. The clusters with high SI index are well matched to its own cluster. It is clearly seen that the SI index is quite high for x-means on daily, weekly, monthly, and randomly selected TU data, when the cluster number is six, whereas hierarchical clustering achieved high SI indexing for cluster number six in all cases except randomly selected TUs. Again, in the Gaussian mixture algorithm, SI values are not concentrated for a single cluster number, therefore it is hard to discover a cluster number and their compactness. These internal clustering validation results shows that the selected optimal number of clusters is appropriate and achieved suitable indexing outcomes consistently for x-means than other clustering algorithm. These clustering behaviours results for the developed AFDD were all further verified across all tested HVAC TUs with the help of expert building engineers from Demand Logic.



(a) Weekly Cluster Radar



(b) Monthly Cluster Radar



(c) Random Cluster Radar

Figure 11: Cluster wise feature distribution: (a) weekly TU data, (b) monthly TU data, and (c) randomly selected TU data

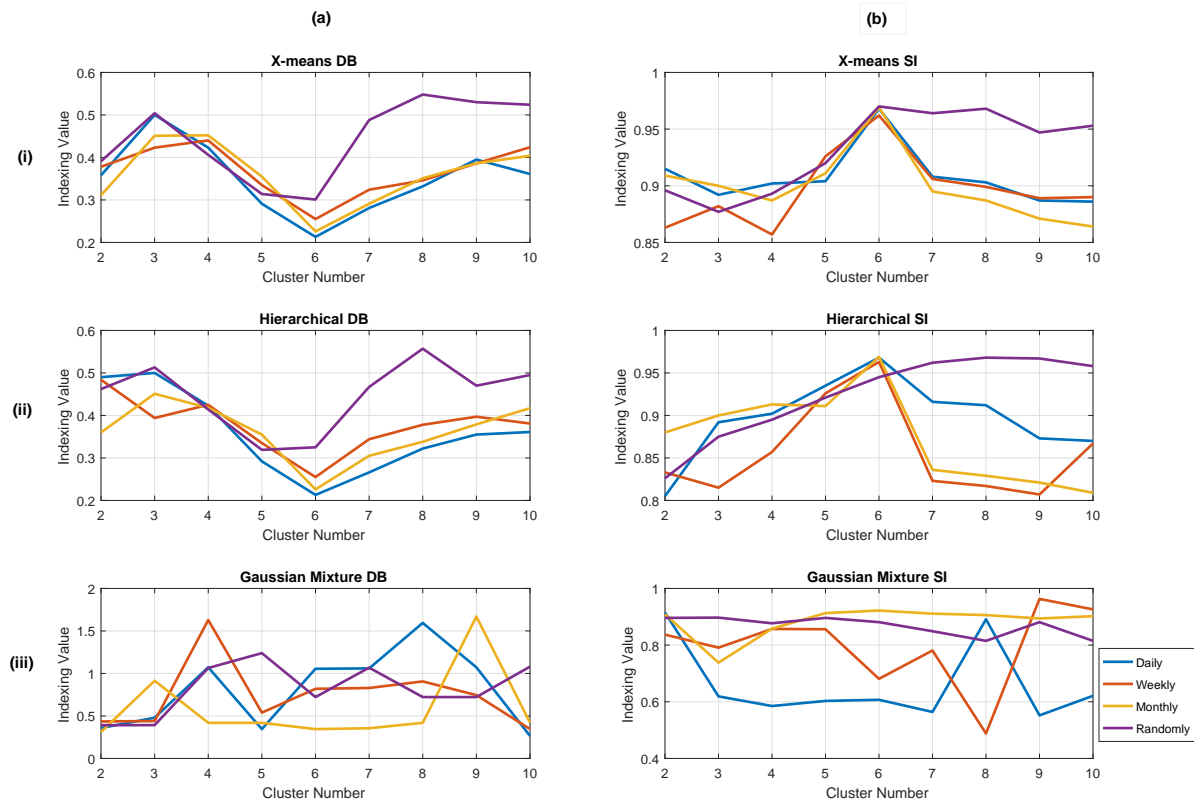


Figure 12: Clustering Validation and comparison

496 *5.2. Classification Result Analysis*

497 The clustering outcomes are used as pre-processing step for classification of TU data. Therefore,  
 498 the TUs are labelled using the clustering outcomes to make an automated fault diagnosis and  
 499 predictive system for buildings. In this phase the classification is performed by employing MC-  
 500 SVM, where the dataset is categorized and labelled into six different classes for diagnosing diverse  
 501 behaviour of faulty and non-faulty TUs (tabulated in Table 2).

502 Here, the experiment is conducted by dividing the TU dataset in 10%, 20%, 30% for training,  
 503 and 90%, 80%, 70% respectively for testing purposes. The number of objects (NOB) or TUs are 656.  
 504 Statistical evaluation of performance parameters like, accuracy, precision, and recall are evaluated  
 505 and recorded in Table 3. The highest precision and recall value obtained from 10% training and 90%  
 506 testing data (marked in bold) in all the cases using MC-SVM. This algorithm achieved an excellent  
 507 performance with 99.3% of precision in randomly selected data, which signifies a high positive  
 508 predictive value for all predicted TUs. Also observed that the performance increased when the  
 509 training data volume is being increased. The highest recall 96.3% is achieved in case of randomly  
 510 selected data, which directs the relevant prediction of TUs with a very high accuracy. Thus,  
 511 experimental result signifies that the algorithm can make fault predictions about TU behaviour  
 512 with the help of very few amount (only 10% is enough) of training data.

513 Confusion matrixes are set to concentrate on the type of TUs that are assigned in wrong cate-  
 514 gory by the algorithm. Four confusion matrices are shown in Figure 13. The matrices are prepared  
 515 based on the highest accuracy obtained by MC-SVM (where only 10% training data are used).  
 516 Each element in this matrix is the number of test items with true class in row wise and predicted  
 517 class in column wise. The correctly classified objects are plotted diagonally (marked in blue color)

Table 3: Classification results by MC-SVM

Observations		10%	20%	30%
Daily	NOB	656	595	536
	Precision	<b>0.983</b>	0.982	0.979
	Recall	<b>0.921</b>	0.913	0.897
Weekly	NOB	3262	2970	2672
	Precision	<b>0.979</b>	0.978	0.977
	Recall	<b>0.905</b>	0.902	0.896
Monthly	NOB	12944	11705	10643
	Precision	<b>0.988</b>	0.988	0.987
	Recall	<b>0.943</b>	0.942	0.938
Randomly	NOB	29744	27002	24339
	Precision	<b>0.993</b>	0.992	0.992
	Recall	<b>0.965</b>	0.964	0.964

518 and misclassified objects are marked in light blue. Though the overall performance of the pro-  
519 posed algorithm is good, still some characteristics of TUs confound the classifier which causes the  
520 misidentification. It is clearly seen that the objects of class-1 are misidentified mostly in case of  
521 daily (Figure 13(a)) and class-2 in case of weekly (Figure 13(b)) analysis. In Figure 13(a) and  
522 13(b), 6 and (11+7+3+17)=38 objects are misidentified because, the TUs belong to these classes  
523 are distinct by the cooling and heating temperature but similar in nature with respect to power.  
524 In case of monthly and randomly (Figure 13(c) and 13(d)) data, misclassifications occurred mostly  
525 from class-0, whereas this class holds the good behaving and distinct TUs with respect to temper-  
526 ature and power consumption. A huge number of objects belong to this class and numerically the  
527 differences between the objects are very small. Therefore, the classifier is over fitted and overreacted  
528 to the slight fluctuations in the feature values.

		Predicted						
		n=656	Class 0	Class 1	Class 2	Class 3	Class 4	Class 5
Actual	Class 0	33	2	0	0	0	0	0
	Class 1	0	431	0	1	0	0	0
	Class 2	0	2	58	0	0	0	0
	Class 3	0	1	0	51	0	0	0
	Class 4	0	0	4	0	35	0	0
	Class 5	0	1	0	0	0	0	37

(a) Daily TUs

		Predicted						
		n=3262	Class 0	Class 1	Class 2	Class 3	Class 4	Class 5
Actual	Class 0	176	2	11	1	1	1	1
	Class 1	0	221	7	0	0	1	1
	Class 2	1	2	1929	0	2	0	0
	Class 3	0	0	0	220	0	7	0
	Class 4	2	1	3	0	348	0	0
	Class 5	0	0	17	0	8	301	0

(b) Weekly TUs

		Predicted						
		n=12944	Class 0	Class 1	Class 2	Class 3	Class 4	Class 5
Actual	Class 0	7550	6	2	7	8	21	0
	Class 1	9	1279	12	3	3	0	0
	Class 2	26	2	811	6	0	0	0
	Class 3	6	1	1	838	2	1	0
	Class 4	4	1	1	2	1079	0	0
	Class 5	6	4	8	7	3	1235	0

(c) Monthly TUs

		Predicted						
		n=29744	Class 0	Class 1	Class 2	Class 3	Class 4	Class 5
Actual	Class 0	14364	0	13	0	5	4	0
	Class 1	0	3252	2	11	4	2	0
	Class 2	23	2	2139	5	1	0	0
	Class 3	46	8	0	4311	13	0	0
	Class 4	24	0	2	11	3188	0	0
	Class 5	21	1	6	2	6	2278	0

(d) Randomly Selected TUs

Figure 13: Confusion matrix by MC-SVM

529 Further this experimental result is compared with another classification method, k-nearest neigh-  
530 bour (KNN) [42], which is a well-established, non-parametric method for classification that assigns  
531 the class number to an object based on the nearest distance of its neighbours. Here, k is chosen as  
532 1 and 3 and the results are shown in Table 4. Table 4 shows the precision and recall outcomes for  
533 1NN and 3NN with 10%, 20% and 30% training samples. Thus, it is observed from the result table  
534 that 30% training sample is required for 1NN and 3 NN to produce maximum precision and recall

535 values, except in case of 1NN for daily analysis 20% training data is needed for high performance.  
 536 Thus, it is determined that MC-SVM provides high precision and recall with less number of training  
 537 data than KNN classifier.

Table 4: Precision and recall comparison of 1NN and 3NN

Observations		10%		20%		30%	
		1NN	3NN	1NN	3NN	1NN	3NN
Daily	NOB	654	656	588	593	525	533
	Precision	0.945	0.916	0.957	0.944	0.949	0.961
	Recall	0.774	0.686	0.818	0.772	0.786	0.829
Weekly	NOB	3265	3274	2966	2964	2680	2697
	Precision	0.957	0.950	0.969	0.967	0.972	0.973
	Recall	0.818	0.792	0.863	0.855	0.877	0.877
Monthly	NOB	12942	12968	11693	11721	10600	10621
	Precision	0.968	0.967	0.971	0.975	0.974	0.976
	Recall	0.861	0.855	0.871	0.886	0.885	0.890
Randomly	NOB	29758	29766	26912	26896	24411	24383
	Precision	0.969	0.970	0.974	0.976	0.979	0.977
	Recall	0.865	0.865	0.882	0.891	0.904	0.898

538 The precision and recall values are plotted in Figure 14 to compare the performance of MC-SVM,  
 539 1NN, and 3NN for 10%, 20%, and 30% training set. Precision and recall are shown in blue and  
 540 yellow colour respectively. It is observed that MC-SVM achieved higher precision and recall than  
 541 1NN and 3NN for all time spans. Therefore, the performance of the MC-SVM shows the effective  
 542 diagnosis of faulty and non-faulty HVAC TUs is possible with the help of supervised learning.

543 The fault diagnosis results by MC-SVM algorithm for all the experimented TUs described above  
 544 coincide with the fact that indicates this method employed for any types of faulty and non-faulty  
 545 HVAC TUs diagnosis is effective.

### 546 5.3. Discussion

547 Real TU behaviour is analysed remotely in this work, where temperature set point and corre-  
 548 sponding power consumption are considered as the parameters for characteristics. These parameters  
 549 enable a story to form around the HVAC and its direct environment, i.e. providing real data on the  
 550 building under test and enabling managers to investigate faulty HVACs not all HVACs. Three dis-  
 551 tinct fault and three non-fault clusters have been remotely identified and classified. From the AFDD  
 552 results, it can be concluded that faulty behaviour can be automatically and remotely detected and  
 553 understood. Subsequently useful and exact information can be delivered to those managing the  
 554 TUs in question. Using this vital new information an investigator can then identify if it is the  
 555 environment (set-point issues) or the particular HVAC creating the fault?

556 Additionally predictive fault finding can be achieved using the classification results presented,  
 557 thus managers can ensure timely interventions. In some cases where a fault is assumed, in actual  
 558 fact the TUs in question once checked are not "broken" but for example have had their temperature  
 559 set points set too high or low for their environmental setting, making it difficult for those TUs to  
 560 achieve set point temperature leading to "faulty" behaviour displays. Additionally, too narrow  
 561 dead band settings (difference between high and low set points) ranges cause many potential faulty  
 562 behaviour. External influences such as weather conditions, sunlight, photocopiers, fridges, manual  
 563 set point changes (based on personal preferences), open windows, etc. are not considered for both  
 564 the set point and dead band levels estimation. Usually set point changes in situations above can  
 565 be triggered by the building occupants depending upon their desired comfort levels and the effect

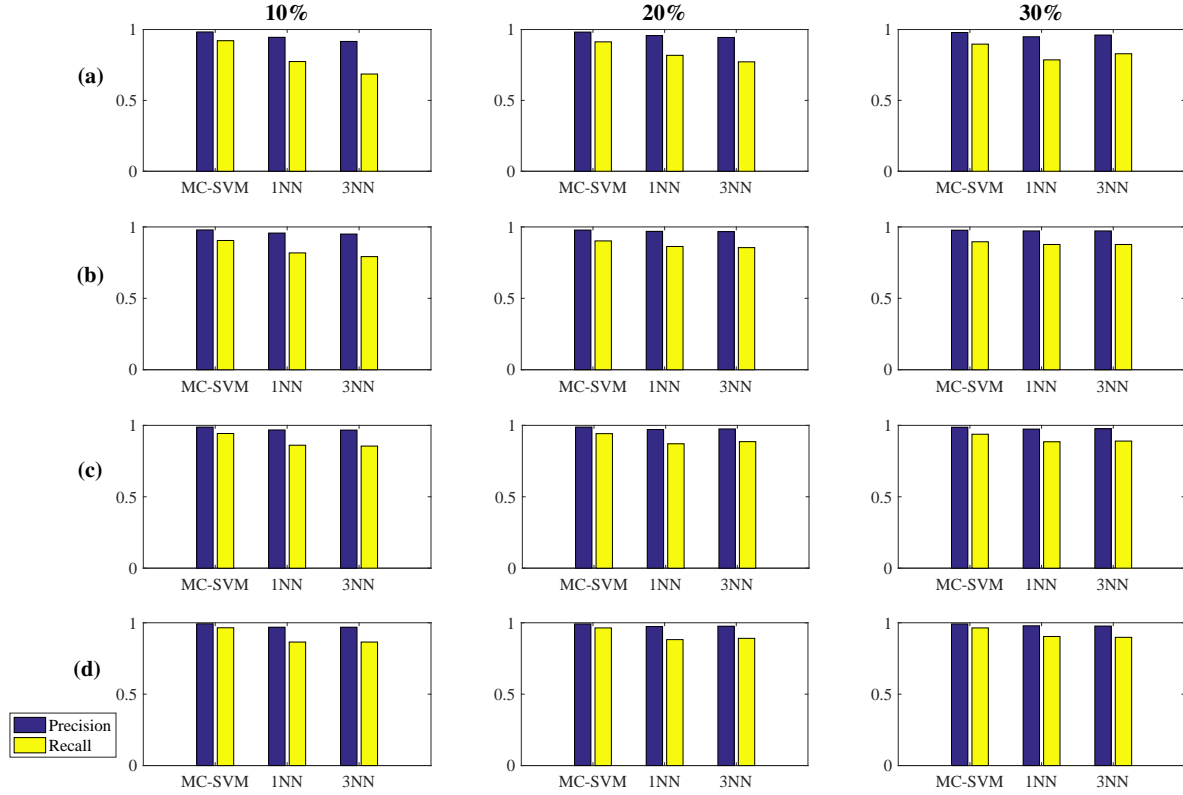


Figure 14: Precision and recall value analysis for TU data of (a) Daily, (b) Weekly, (c) Monthly, and (d) Randomly

566 of such request on TU behaviour is observable. Affected TUs subsequently demand excess power  
 567 but will be unable to maintain the control strategies requested. Importantly the TUs in this case  
 568 are not always defective but simply trying to achieve unattainable goals. Thus, energy and OPEX  
 569 savings can be quickly made by addressing these external issues and the AFDD proposed provides  
 570 this assistance.

## 571 6. Conclusion and Future Work

572 A novel feature extraction technique is presented to extract temperature and power associated  
 573 features from high-dimensional and unstructured TU data. These features provide a good approxi-  
 574 mation for the TU characteristics and are tested on large number of TUs. An unsupervised learning  
 575 technique was employed to identify distinct TU behavioural patterns and discriminate the faulty  
 576 and non-faulty TUs. Subsequently, a classification method was applied to predict and diagnose the  
 577 faults from a building automatically. Due to the more realistic implementation i.e. lack of knowl-  
 578 edge of sensor location, weather data, and the occupancy information, it is difficult to detect and  
 579 diagnose the cause of faults effectively here, though the excellent accuracy of the proposed method  
 580 signifies the real world effectiveness of the work.

581 This experiment has been tested on more than 39,000 TUs and gathered the ground truth  
 582 information. Augmenting this work includes further tests on TUs where faults such as, improper  
 583 dead bands and set point temperatures have been identified using AFDD and rectified. It could be  
 584 used to predict faults on more recent data by using semi-supervised learning techniques. Further

585 analysis will be based on the external and internal causes of the faults by the help of building experts  
586 towards fully remote fault diagnosis, so that, the quality research can provide useful and meaningful  
587 conclusions. Additionally, deep learning based methods will be explored for on-line training and  
588 testing purposes to enact AFDD in a real-time manner. The method developed and deployed for  
589 this paper is limited to a specific type of TU (Fan Coil Unit) of a single building, but it will be  
590 extended to different types of TUs such as air handling unit (AHU), variable air volume (VAV) and  
591 chilled beam etc.

## 592 7. Acknowledgement

593 This work has been carried out as a part of the Innovate UK funded research project (EP/M506734/1)  
594 Energy Management & Analysis Exploiting Existing BEMS Infrastructure & Data and the authors  
595 are grateful to the Demand Logic team for providing us with the BEMS data, verification, invaluable  
596 information and feedback on building services and related performance issues.

## 597 References

- 598 [1] D. Kolokotsa, The role of smart grids in the building sector, *Energy and Buildings* 116 (2016)  
599 703–708.
- 600 [2] C. Talon, R. Martin, Next generation building energy management system - new opportunities  
601 and experiences enabled by intelligent equipment, Technical report, Navigant Research (2Q  
602 2015).
- 603 [3] P. Usoro, I. Schick, S. Negahdaripour, An innovation-based methodology for hvac system fault  
604 detection, *Journal of dynamic systems, measurement, and control* 107 (4) (1985) 284–289.
- 605 [4] D. Anderson, L. Graves, W. Reinert, J. Kreider, J. Dow, H. Wubbena, A quasi-real-time expert  
606 system for commercial building hvac diagnostics, *ASHRAE Transactions (American Society of  
607 Heating, Refrigerating and Air-Conditioning Engineers);(USA)* 95 (CONF-890609).
- 608 [5] S.-H. Cho, H.-C. Yang, M. Zaheer-Uddin, B.-C. Ahn, Transient pattern analysis for fault  
609 detection and diagnosis of hvac systems, *Energy Conversion and Management* 46 (18) (2005)  
610 3103–3116.
- 611 [6] S. Shaw, L. Norford, D. Luo, S. Leeb, Detection and diagnosis of hvac faults via electrical load  
612 monitoring, *HVAC&R Research* 8 (1) (2002) 13–40.
- 613 [7] T. Salsbury, A temperature controller for VAV air-handling units based on simplified physical  
614 models, *HVAC&R Research* 4 (3) (1998) 265–279.
- 615 [8] T. Salsbury, R. Diamond, Fault detection in hvac systems using model-based feedforward  
616 control, *Energy and Buildings* 33 (4) (2001) 403–415.
- 617 [9] L. K. Norford, J. A. Wright, R. A. Buswell, D. Luo, C. J. Klaassen, A. Suby, Demonstration of  
618 fault detection and diagnosis methods for air-handling units, *HVAC&R Research* 8 (1) (2002)  
619 41–71.
- 620 [10] P. Haves, M. Kim, Model-based automated functional testing methodology and application to  
621 air-handling units (2005) 979–989.

- 622 [11] S. Wu, J.-Q. Sun, A physics-based linear parametric model of room temperature in office  
623 buildings, *Building and Environment* 50 (2012) 1–9.
- 624 [12] S. Wu, J. Sun, Multi stage regression linear parametric models of room temperature in office  
625 buildings, *Building and Environment* 56 (2012) 69–77.
- 626 [13] L. H. Chiang, R. D. Braatz, E. L. Russell, *Fault detection and diagnosis in industrial systems*,  
627 Springer Science & Business Media, 2001.
- 628 [14] J. Shiozaki, F. Miyasaka, A fault diagnosis tool for hvac systems using qualitative reasoning  
629 algorithms, in: *Proceedings of the Building Simulation*, Vol. 99, 1999.
- 630 [15] J. Schein, S. T. Bushby, N. S. Castro, J. M. House, A rule-based fault detection method for  
631 air handling units, *Energy and buildings* 38 (12) (2006) 1485–1492.
- 632 [16] J. Schein, S. T. Bushby, N. S. Castro, J. M. House, Results from field testing of air handling  
633 unit and variable air volume box fault detection tools.
- 634 [17] A. Dexter, J. Pakanen, et al., Demonstrating automated fault detection and diagnosis methods  
635 in real buildings, Technical Research Centre of Finland (VTT), 2001.
- 636 [18] J. Schein, S. T. Bushby, A hierarchical rule-based fault detection and diagnostic method for  
637 hvac systems, *HVAC&R Research* 12 (1) (2006) 111–125.
- 638 [19] S. R. West, Y. Guo, X. R. Wang, J. Wall, Automated fault detection and diagnosis of hvac  
639 subsystems using statistical machine learning, in: *12th International Conference of the Inter-  
640 national Building Performance Simulation Association*, 2011.
- 641 [20] E. Alpaydin, *Introduction to machine learning*, MIT press, 2014.
- 642 [21] C.-F. Chien, S.-L. Chen, Y.-S. Lin, Using bayesian network for fault location on distribution  
643 feeder, *IEEE Transactions on Power Delivery* 17 (3) (2002) 785–793.
- 644 [22] W.-Y. Lee, J. M. House, C. Park, G. E. Kelly, Fault diagnosis of an air-handling unit using  
645 artificial neural networks, *Transactions American Society of Heating Refrigerating and Air  
646 Conditioning Engineers* 102 (1996) 540–549.
- 647 [23] J. Liang, R. Du, Model-based fault detection and diagnosis of hvac systems using support  
648 vector machine method, *International Journal of refrigeration* 30 (6) (2007) 1104–1114.
- 649 [24] A. L. Dexter, D. Ngo, Fault diagnosis in air-conditioning systems: a multi-step fuzzy model-  
650 based approach, *HVAC&R Research* 7 (1) (2001) 83–102.
- 651 [25] D. Li, G. Hu, C. J. Spanos, A data-driven strategy for detection and diagnosis of building  
652 chiller faults using linear discriminant analysis, *Energy and Buildings* 128 (2016) 519–529.
- 653 [26] R. Isermann, *Fault-diagnosis applications: model-based condition monitoring: actuators,  
654 drives, machinery, plants, sensors, and fault-tolerant systems*, Springer Science & Business  
655 Media, 2011.
- 656 [27] Y. Zhao, S. Wang, F. Xiao, Pattern recognition-based chillers fault detection method using  
657 support vector data description (SVDD), *Applied Energy* 112 (2013) 1041–1048.

- 658 [28] A. Beghi, R. Brignoli, L. Cecchinato, G. Menegazzo, M. Rampazzo, F. Simmini, Data-driven  
659 fault detection and diagnosis for hvac water chillers, *Control Engineering Practice* 53 (2016)  
660 79–91.
- 661 [29] A. Widodo, B.-S. Yang, Support vector machine in machine condition monitoring and fault  
662 diagnosis, *Mechanical systems and signal processing* 21 (6) (2007) 2560–2574.
- 663 [30] M. Dey, M. Gupta, M. Turkey, S. Dudley, Unsupervised learning techniques for HVAC terminal  
664 unit behaviour analysis, in: *The 2017 IEEE International Conference on Smart City Innovations*  
665 (*IEEE SCI 2017*), San Francisco, USA, 2017.
- 666 [31] K. J. Åström, T. Hägglund, *Advanced PID control*, ISA-The Instrumentation, Systems and  
667 Automation Society, 2006.
- 668 [32] Z. Huang, Extensions to the k-means algorithm for clustering large data sets with categorical  
669 values, *Data mining and knowledge discovery* 2 (3) (1998) 283–304.
- 670 [33] D. L. Davies, D. W. Bouldin, A cluster separation measure, *IEEE transactions on pattern*  
671 *analysis and machine intelligence* (2) (1979) 224–227.
- 672 [34] P. J. Rousseeuw, Silhouettes: a graphical aid to the interpretation and validation of cluster  
673 analysis, *Journal of computational and applied mathematics* 20 (1987) 53–65.
- 674 [35] K. Crammer, Y. Singer, On the algorithmic implementation of multiclass kernel-based vector  
675 machines, *Journal of machine learning research* 2 (Dec) (2001) 265–292.
- 676 [36] S. P. Rana, M. Dey, H. Siddiqui, G. Tiberi, M. Ghavami, S. Dudley, UWB localization employ-  
677 ing supervised learning method, in: *IEEE International Conference on Ubiquitous Wireless*  
678 *Broadband ICUWB2017*, Salamanca, Spain, 2017.
- 679 [37] G. Bello-Orgaz, J. J. Jung, D. Camacho, Social big data: Recent achievements and new chal-  
680 lenges, *Information Fusion* 28 (2016) 45–59.
- 681 [38] M. Zaharia, M. Chowdhury, M. J. Franklin, S. Shenker, I. Stoica, Spark: Cluster computing  
682 with working sets., *HotCloud* 10 (10-10) (2010) 95.
- 683 [39] R. S. Xin, J. Rosen, M. Zaharia, M. J. Franklin, S. Shenker, I. Stoica, Shark: Sql and rich  
684 analytics at scale, in: *Proceedings of the 2013 ACM SIGMOD International Conference on*  
685 *Management of data*, ACM, 2013, pp. 13–24.
- 686 [40] Á. B. Hernández, M. S. Perez, S. Gupta, V. Muntés-Mulero, Using machine learning to optimize  
687 parallelism in big data applications, *Future Generation Computer Systems*, 2017, Elsevier.
- 688 [41] I. H. Witten, E. Frank, M. A. Hall, C. J. Pal, *Data Mining: Practical machine learning tools*  
689 *and techniques*, Morgan Kaufmann, 2016.
- 690 [42] Z. Zhou, C. Wen, C. Yang, Fault isolation based on k-nearest neighbor rule for industrial  
691 processes, *IEEE Transactions on Industrial Electronics* 63 (4) (2016) 2578–2586.